大 气 科 学
Chinese Journal of Atmospheric Sciences
Volume 11, No. 1

An Air-Sea Feedback Mechanism for Quasi-Geostrophic Water Movement Near a Fast Shelf-Ice Edge With a Small Curvature

P. C. Chu

(Department of Oceanography, Naval Postgraduate School, Monterrey, California)

An air-sea coupled model developed in this paper is intended to depict the generation of unstable coastal water waves near a fast shelf-ice edge with small curvature. Without any external forcing of the system, the unstable modes are excited by the air-sea feedback mechanism. Thermally forced surface winds, generated by a surface temperature gradient that is related to the vertical displacement of the pycnocline, in turn produce a surface water current that further changes the vertical displacement of the pycnocline. The model consists of two elements: thermally forced surface air flow and mechanically driven coastal water waves (Clarke). The two components are linked through the surface temperature gradient and surface wind stress. The coupled air-sea model is solved as an eigenvalue problem. It is found that the iceward convex ice-edge, relatively thin ice, and small upper-layer water depth favor the generation of very unstable modes. The influence of the coupling on the wave velocity is also discussed.

I. INTRODUCTION

Clarke (1978) discussed in detail the wind-driven quasi-geostrophic water movement near a fast shelf-ice, i.e., glacial ice which is attached to a land mass. Water motion near the shelf-ice edge is generated not only by a stress curl mechanism, but also by a blocking action as in the coastal case. The quasi-geostrophic motion can be described by wind-forced trapped long waves which propagate along the ice-edge with the ice on their left (right) in the Southern (Northern) Hemisphere (Clarke, 1978). In Clarke's model the wind stress is taken as a known function (external forcing). However, in this paper the surface winds are deter-

Received January 20, 1987

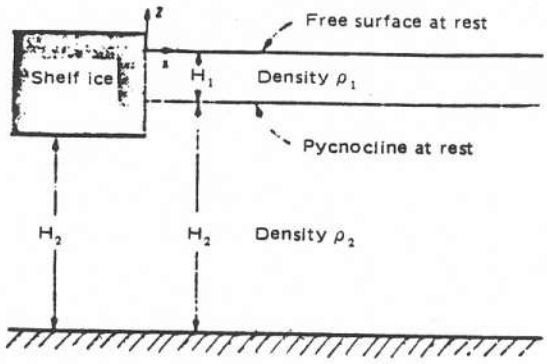

FIGURE 1. Diagrammatic representation of two-layer shelf-ice model (Clarke, 1978).

mined by the surface temperature gradient which is related to the vertical displacement of the pycnocline, h. The air-sea feedback model depicted in the subsequent sections is intended to change the Clarke equation into a homogeneous equation for h, and then treat it as an eigenvalue problem.

II. AIR-SEA COUPLED SYSTEM

Clarke (1978) developed a two layer shelf-ice model to discuss wind-driven quasi-geostrophic water movement near fast shelf-ice edges with small curvature (Fig. 1). The small curvature means that the radius of curvature of ice-edge at any point is much greater than the baroclinic radius of deformation. Such curvature effects can be examined by using normal and tangential coordinates (n, s). Here, n is defined as the distance seaward from the ice-edge, and s is the distance along the ice-edge from the origin. The curvature $\kappa(n)$ is defined to be positive (negative) when the ice edge is convex seaward (iceward). For small curvature of ice edges the upward displacement of the pycnocline h* is

$$h^*(n, s, t) = h(s,t)\, e^{-n/a(1 + \kappa/2)} + O(\kappa^2), \tag{1}$$

where h(s, t) satisfies

$$\frac{\partial h}{\partial t} - \gamma \frac{\partial h}{\partial s} = \frac{\gamma(\mu - 1)}{\mu \rho_1 H_1 g'} \left[f \vec{e}_s \cdot \vec{\tau} + \vec{e}_n \cdot \frac{\partial \vec{\tau}}{\partial t} \right], \tag{2}$$

with

$$\gamma = \frac{\mu}{\mu - 1}\left[1 - \kappa\left(\frac{1}{2} + \frac{1}{\mu - 1}\right)\right] af + O(\kappa^2), \tag{3}$$

$$\mu = \frac{H_2 \Delta H}{2HH_1}\left[1 + \left(\frac{H}{H_2'}\right)^2\right] - \frac{\Delta H_2 H}{2H_2 H_1}\left[1 + \left(\frac{H_2}{H_2'}\right)^2\right], \tag{4}$$

where H_1, H_2 are the upper- and lower-layer depths; a is the radius of deformation of the baroclinic mode; H_2' is the lower-layer depth under the ice; H is the total water depth; $\Delta H_2 = H_2 - H_2'$, and $\Delta H = H - H_2'$; κ is the ice-edge curvature non-dimensionalized with respect to the reciprocal of the baroclinic radious of deformation; $\vec{\tau}$ is the wind stress; $\vec{e}_n$ and $\vec{e}_s$ are the unit vectors in the direction of increasing n and s, respectively; g′ is reduced gravity $g(\rho_2 - \rho_1)/\rho_2$. Here g is acceleration due to gravity, and ρ_1 and ρ_2 are the upper- and lower-layer densities.

The sea surface temperature (SST) anomaly T_s' caused by pycnocline fluctuation is assumed to be proportional to h* in the following form

$$T_s' = \frac{\Delta T}{H_1} h^* = \frac{\Delta T}{H_1} h\, e^{-n/a(1 + \kappa/2)}, \tag{5}$$

which means that the coastal upwelling ($h > 0$) near a fast shelf-ice will give rise to the warm anomaly. Here $\Delta T = T_2 - T_1 > 0$, is a temperature difference between the lower- and upper-layers. Such a differential SST anomaly generates a thermally forced wind. Chu (1986abc) developed a coupled air-ice-ocean model for the marginal ice zone (MIZ) to show that thermally forced surface winds blow

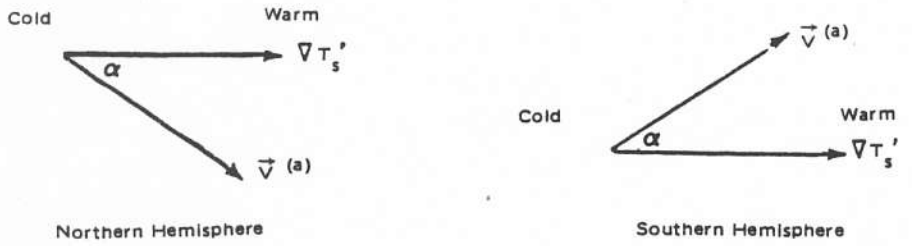

FIGURE 2. Relationship between thermally forced surface wind and the surface temperature gradient.

across the isotherms from cold to warm regions with some deflection due to the Earth rotation. The deflection angle α (Fig. 2) depends on the atmospheric Richardson number (Chu, 1986c), and the wind speed is proportional to $|\nabla T_s'|$, which is computed by

$$|\nabla T_s'| \sim \frac{\partial T_s'}{\partial n} = -\frac{\Delta T}{H_1}\,\frac{h}{a}\left(1+\frac{\kappa}{2}\right) e^{-n/a(1+\kappa/2)}. \tag{6}$$

Therefore, the thermally forced surface winds are estimated by

$$v_s^{(a)} = \alpha_s h\, e^{-n/a(1+\kappa/2)}, \qquad v_n^{(a)} = -\alpha_n h\, e^{-n/a(1+\kappa/2)}. \tag{7}$$

The parameters α_s and α_n are defined by

$$\alpha_s \equiv b\,\frac{\Delta T}{H_1}\,\frac{(1+\kappa/2)}{a}\sin\alpha, \tag{8}$$

$$\alpha_n \equiv b\,\frac{\Delta T}{H_1}\,\frac{(1+\kappa/2)}{a}\cos\alpha, \tag{9}$$

where b is a proportionality constant which represents the wind speed thermally forced by a unity of surface temperature gradient. According to Defant (1950), 1°C/100 km surface temperature gradient can generate about 2 m/s surface wind. Hence, we take

$$b = \frac{2\ \text{m/s}}{1^{\circ}\text{C}/100\ \text{km}}.$$

Surface wind stress $\vec{\tau}$ is then obtained by

$$\tau_s = \rho_a C_a v_s^{(a)}, \qquad \tau_n = \rho_a C_a v_n^{(a)}, \tag{10}$$

where C_a is the dimensional (m/s) air drag coefficient. Substituting (10) into (2) and using (7) lead to the following equation

$$\left[1+\frac{\gamma(\mu-1)\omega\,\alpha_n}{\mu g'}\right]\frac{\partial h}{\partial t} - \gamma\frac{\partial h}{\partial s} - \frac{f\gamma(\mu-1)\omega\,\alpha_s}{\mu g'}\,h = 0, \tag{11}$$

where

$$\omega \equiv \frac{\rho_a C_a}{\rho_1 H_1}.$$

The amplitude of the pycnocline displacement h is then governed by a free, first-order wave equation with two air-sea coupling coefficients α_s and α_n.

III. WAVE SOLUTION

Let the solution of the basic equation (11) have the following wave form:

$$h(s, t) = A\, e^{i(\sigma t - ms)}. \tag{12}$$

Substituting (12) into (11) gives the dispersion relation

$$\sigma = -\frac{\gamma\mu g' m}{\mu g' + \gamma(\mu - 1)\omega\, \alpha_n} - \frac{f\gamma(\mu - 1)\omega\, \alpha_s}{\mu g' + \gamma(\mu - 1)\omega\, \alpha_n}\, i. \tag{13}$$

Wave speed is computed by

$$c = \frac{\mathrm{Re}(\sigma)}{m} = -\frac{\gamma\mu g'}{\mu g' + \gamma(\mu - 1)\omega\, \alpha_n}. \tag{14}$$

Growth rate is given by

$$-\mathrm{Im}(\sigma) = \frac{f\gamma(\mu - 1)\, \omega\, \alpha_s}{\mu g' + \gamma(\mu - 1)\omega\, \alpha_n}. \tag{15}$$

IV. STABILITY CRITERION

The standard values of parameters are given in Table 1. The imaginary part of frequency σ_i and the wave speed c are computed for different values of κ, H_2'/H_2, and H_1/H_2. Figure 3 shows the surface $\sigma_i = 0$ or $c = 0$ in the three-dimensional space (κ, H_2'/H_2, H_1/H_2). The surface of $\sigma_i = 0$ is coincident with the surface $c = 0$. Therefore, this surface divides the space into two parts cor-

TABLE 1
The Standard Model Parameters

$a = 10$ km,	$H_2 = 1$ km,	$C_a = 1.5 \times 10^{-2}$ m/s,	$\Delta T = 5°C$,
$\rho_a = 1.29$ kg/m^3,	$\rho_1 = 10^3$ kg/m^3,	$\rho_2 = 1000.5$ kg/m^3,	
$\alpha = \tan^{-1}(0.6)$,	$b = 2 \times 10^5$ m^{2}s^{-1}°C^{-1}.		

responding to a growing and negative propagation mode, and a decaying and positive propagation mode. Here, the negative (positive) propagation means that the wave propagates in the direction with the ice-edge on the right (left) in the Northern Hemisphere, and with the ice-edge on the left (right) in the Southern Hemisphere.

Figure 3 indicates the following facts. (a) A negative (positive) propagating, self-excited coastal wave is growing (decaying). (b) For an iceward convex ice-edge ($\kappa < 0$) the coastally trapped waves are all growing. (c) For a seaward convex ice-edge ($\kappa > 0$) the waves are growing in a thick-ice region ($H_2'/H_2 < 0.7$) and decaying in a thin ice region ($H_2'/H_2 > 0.7$).

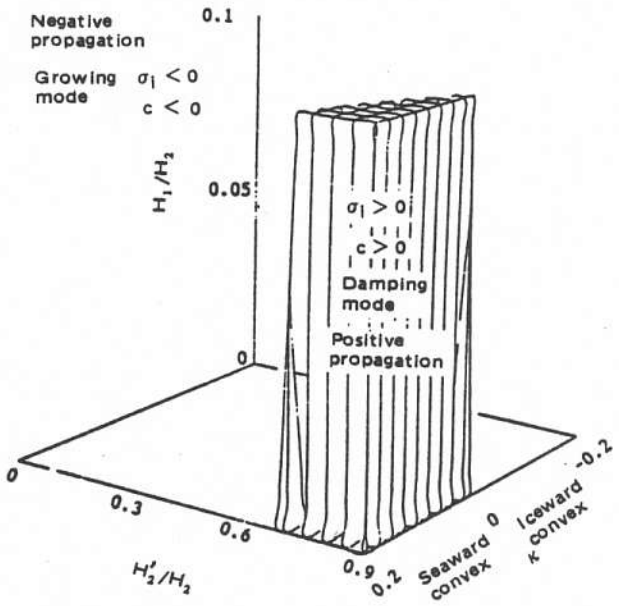

FIGURE 3. Separation of growing (decaying) and positively (negatively) propagating modes.

TABLE 2

Some Typical Values of Growth Rate (Doubling Tim or an Iceward Convex Ice-Edge ($\kappa = -0.2$)

	Thin ice ($H_2'/H_2 = 0.8$)	Thick ($H_2'/$ = 0.5)	Very thick ice ($H_2'/H_2 = 0.1$)
Small upper-layer depth ($H_1/H_2 = 0.01$)	$10^{-5}s^{-1}$ (19.3 hr)	10 (8. days)	$0.316\times10^{-6}s^{-1}$ (25.4 days)
Large upper-layer depth ($H_1/H_2 = 0.09$)	$0.6\times10^{-7}s^{-1}$ (134 days)	10 (2. 5 yr.)	$10^{-8}s^{-1}$ (2.196 yr.)

TABLE 3

Some Typical Values of Growth Rate (Doubling Time r Decay Rate (Half-life Period*) for a Seaward Convex Ice-Edg $\kappa = 0.2$)

	Thin ice ($H_2'/H_2 = 0.8$)	Thick e ($H_2'/$ = 0.5)	Very thick ice ($H_2'/H_2 = 0.1$)
Small upper-layer depth ($H_1/H_2 = 0.01$)	$-0.56\times10^{-5}s^{-1}$ (1.43 days)*	1(s^{-1} (8 days)	$0.316\times10^{-6}s^{-1}$ (25.4 days)
Large upper-layer depth ($H_1/H_2 = 0.09$)	$-0.36\times10^{-7}s^{-1}$ (372.2 days)*	10 s^{-1} (2 96 yr.)	$10^{-8}s^{-1}$ (2.196 yr.)

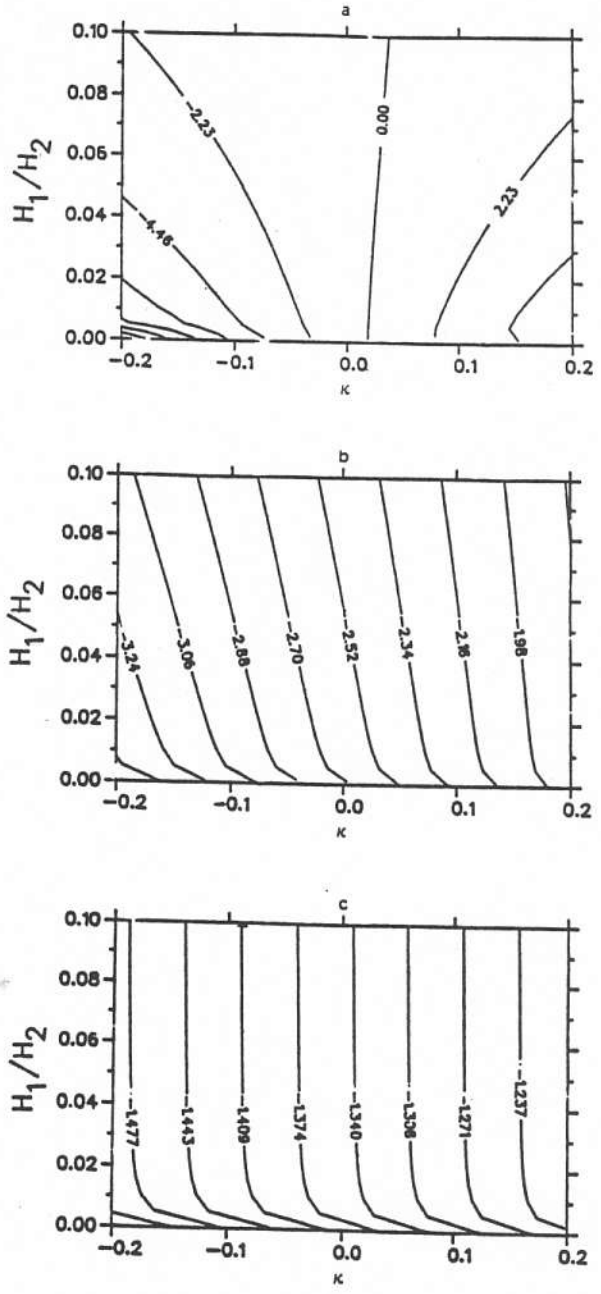

FIGURE 4. Isolines of wave speed (m/sec) for (a) thin ice ($H_2'/H_2 = 0.8$), (b) thick ice ($H_2'/H_2 = 0.5$), and (c) very thick ice ($H_2'/H_2 = 0.1$).

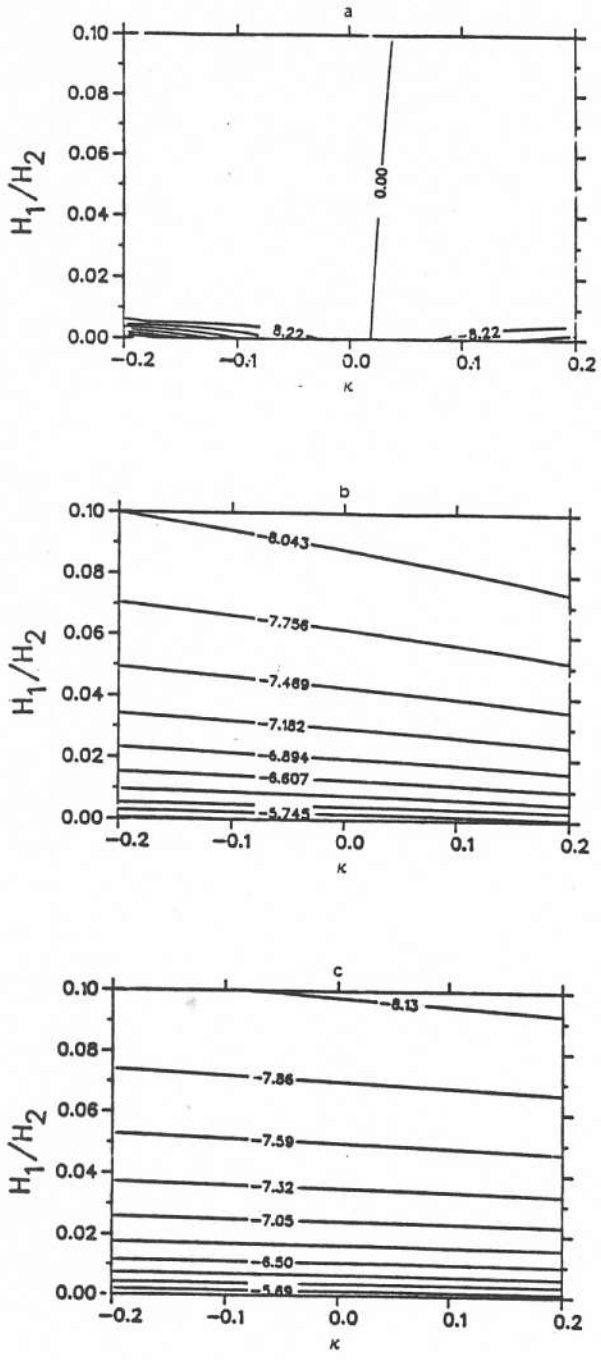

FIGURE 5. Isolines of (a) $-\sigma_l$ ($10^{-6}\,s^{-1}$) for thin ice ($H_2/H_2 = 0.8$), (b) $\log_{10}(-\sigma_l)$ (σ_l in s^{-1}) for thick ice ($H_2/H_2 = 0.5$), and (c) $\log_{10}(-\sigma_l)$ (σ_l in s^{-1}) for very thick ice ($H_2'/H_2 = 0.1$).

V. PROPERTIES OF THE SELF-EXCITED COASTAL TRAPPED WAVES

Figure 4 indicates the isolines of wave speed with H_1/H_2 and κ at three different values of H_2'/H_2 (0.8, 0.5, 0.1). The isoline pattern at $H_2'/H_2 = 0.8$ (thin shelf-ice) is quite different from that at $H_2'/H_2 = 0.5$ and 0.1 (thick and very thick shelf-ice). For thin shelf-ice (Fig. 4a) the curvature of the ice-edge affects the phase velocity dramatically. It not only changes the wave speed, but also alters the direction of propagation. The coastal waves propagate positively (negatively) for convex seaward (iceward) shelf-ice edge. The increase in the absolute value of the ice-edge curvature augments the wave speed. Stronger effects can be seen in the negative area (i.e., convex iceward). For the same curvature, the wave speed decreases with increasing upper-layer depth H_1. However, the isoline patterns at $H_2'/H_2 = 0.5$ and 0.1 (Fig. 4b and c) are very similar. The coastal waves all propagate negatively regardless of whether the ice edge is seaward or iceward convex. The wave speed (absolute value) increases monotonically with decreasing κ. This means that for a given H_1, the coastal wave has its minimum speed at $\kappa = 0.2$ and maximum speed at $\kappa = -0.2$. For a given curvature κ, the wave speed decreases slightly with the increase in the upper-layer depth. Figure 4c also shows that for very thick shelf-ice ($H_2'/H_2 = 0.1$) the wave speed is almost independent of H if H_1 exceeds some critical value near 0.01 H_2.

Figure 5a displays the isolines of the growth rate $-\sigma_i$ in the (H_1/H_2, κ) plane for thin shelf-ice ($H_2'/H_2 = 0.8$). A zero line divides the plane into two parts: growing and decaying modes. The growing (decaying) mode is generated

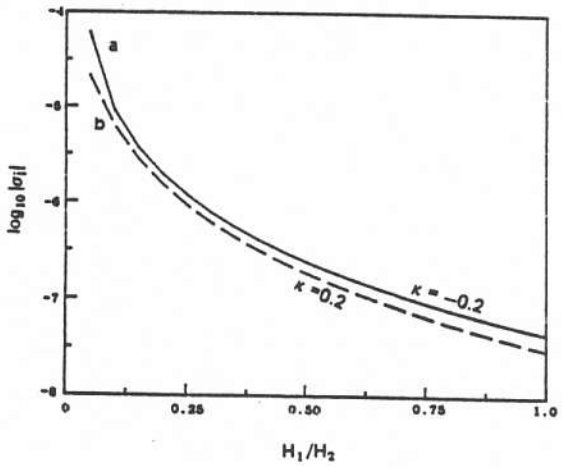

FIGURE 6. Dependence of $\log_{10}|\sigma_i|$ on H_1/H_2 for thin shelf-ice ($H_2'/H_2 = 0.8$): a) $\kappa = -0.2$, and b) $\kappa = 0.2$.

mainly in an iceward (seaward) convex ice-edge. The growth or decay rate decreases rapidly with an increase in upper-layer depth H_1. This is clearly seen in Fig. 6.

Figure 5b and c shows the isolines of the logarithmic growth rate $\log_{10}(-\sigma_i)$ in the $(H_1/H_2, \kappa)$ plane for thick $(H_2/H_2 = 0.5)$ and very thick $(H_2/H_2 = 0.1)$ shelf-ice. The isoline patterns are very similar in these two cases. The growth rate $(-\sigma_i)$ is positive throughout the whole plane and depends more on the upper-layer depth than on the curvature. For small upper-layer depth $H_1/H_2 = 0.01$, the growth rate $(-\sigma_i)$ is around 10^{-6} s^{-1} $(0.316\times10^{-6}$ s$^{-1})$ in thick (very thick) shelf-ice. For a large upper-layer depth $H_1/H_2 = 0.1$, the growth rate $(-\sigma_i)$ becomes as small as 10^{-8} s^{-1} in both the thick and very thick shelf-ice cases.

Figure 6 shows the dependence of logarithmic growth or decay rate $\log_{10}|\sigma_i|$ on H_1/H_2 for thin shelf-ice $(H_2'/H_2 = 0.8)$. In the convex iceward case $(\kappa = -0.2)$, the growth rate drops rapidly with the increase in the upper-layer depth from 10^{-5} s^{-1} (at H/H = 0.01) to 0.6×10^{-7} s^{-1} (at $H_1/H_2 = 0.09$). In the convex seaward case $(\kappa = 0.2)$, the damping rate also decreases rapidly with the increase in upper-layer depth from -0.56×10^{-5} s^{-1} (at $H_1/H_2 = 0.01$) to -0.36×10^{7} s^{-1} (at $H_1/H_2 = 0.09$).

VI. CONCLUSIONS

This air-sea coupled model is intended to depict the generation of unstable coastal water waves without external forcing near a fast shelf-ice edge. The model shows the following results:

(a) Negatively (positively) propagating coastal waves are growing (decaying).

(b) For an iceward convex ice-edge, the coastal waves are all growing. The growth rate decreases rapidly with the increase in the upper-layer depth H_1 and the ice thickness. For a seaward convex ice-edge the coastal waves are growing for thick ice $(H_2'/H_2 < 0.7)$ and decaying for thin ice $(H_2'/H_2 > 0.7)$.

(c) From the investigation of some typical values of growth rate listed in Tables 2 and 3, it is found that iceward convex ice-edge, thin ice, and small upper-layer depth favor the generation of the most unstable modes of the coupled air-sea system, and seaward convex ice-edge, thin ice, and small upper-layer depth favor the damping modes.

(d) The horizontal surface temperature gradient across the ice-edge also generates surface winds, which in turn produce the surface water current and affect the vertical displacement of pycnocline. This effect, which is excluded in this paper, should be taken into consideration in future research.

ACKNOWLEDGEMENTS

This research was supported by Grant ATM 84-02249 from the National Science Foundation.

RÉFERENCES

Chu, P.C., 1986a, "An Instability of Ice-Air Interaction for the Migration of the Marginal Ice Zone," *Geophys. J. Roy. Astron. Soc.*, 86, 863–883.

Chu, P.C., 1986b, "An Ice-Air Feedback Mechanism for the Migration of the Marginal Ice Zone," *MIZEX Bull.*, VII, 54–64.

Chu, P.C., 1986c, "A Possible Air-Ice-Sea Feedback Mechanism for the Formation of Leads or Polynyas," *MIZEX Bull.*, VII, 79–88.

Clarke, A., 1978, "On Wind-Driven Quasi-geostropic Water Movements Near Fast-Ice Edges," *Deep-Sea Research*, 25, 41–51.

Defant, F., 1950, "Theorie der Land- und Seawinde," *Arch. Meteor. Geophys. Biokl.*, 2(A), 404–425.